33RD CONGRESS
OF THE INTERNATIONAL COUNCIL
OF THE AERONAUTICAL SCIENCES
STOCKHOLM, SWEDEN, 4-9 SEPTEMBER, 2022

ICAS 2022 SWEDEN

HANDLING QUALITIES OF A DISTRIBUTED ELECTRIC PROPULSION AIRCRAFT

David Planas[1,2], Carsten Döll[2] & Philippe Pastor[1]

[1]ISAE-SUPAERO
[2]ONERA

Abstract

Reduction of pollution during flight is an everlasting objective in the design of commercial aircraft. Traditional approaches have been oriented towards the increment of bypass ratio (BPR), which has resulted in larger engines. Pursuing this objective, some new approaches have appeared, such as distributed electric propulsion (DEP). Apart from a considerable pollution reduction, DEP leads to new capacities and can increase the efficiency and robustness of future aircraft. The use of DEP creates several aero-propulsive interactions between the wing and the propulsion system, which can be leveraged to achieve increased performance. Several methods exist for the modeling of these aerodynamic-propulsive interactions that occur between the engines and the wing, however, limited research has been done regarding how the handling qualities and the controllability of the aircraft can be affected when modifying the placing and sizing of the different engines and actuators, or when undergoing typical situations like engine failures. This problem will be studied in order to propose a multidisciplinary design methodology for the design of the different actuators and engines at the same time as the control laws for a distributed electrical propelled aircraft.

Keywords: DEP, handling qualities.

1. General Introduction

Distributed Electric Propulsion (DEP) is a propulsion system where the thrust is produced from an array of engines located across the air vehicle. DEP systems, particularly when propellers are mounted in front of the wing, imply a series of particularities that enable new capacities and can provide improved performance over traditional concepts by exploiting certain multidisciplinary interactions, such as Propeller/Wing interaction [1] and other aero-propulsive synergy effects [2], [3].

DEP systems typically use electrically-driven engines that are electrically connected to energy sources. These sources can be a combination of power-producing devices (fuel cells, electric generators coupled with conventional turbines or Auxiliary Power Units) and energy storage devices like batteries. This results in a gain in flexibility when sizing, placing, and operating these devices that can be used to power the synergistic benefits of aero-propulsive interactions [4].

At ONERA research is ongoing with the concepts AMPERE [2] and more ambitiously, DRAGON [3], together with some industrial study contracts. NASA is exploring the concept through prototypes X57 [1] and ECO-150. The university ISAE- SUPAERO has also developed an experimental model called DECOL, useful for the testing and validation of some models.

DEP is an alternative to current conventional propulsion in transport aircraft and it introduces a field of exploration in terms of propulsion, but also in terms of aerodynamics and structure, that requires a global rethinking of aircraft design and operation [5], [6]. It is therefore clear that it is necessary to understand the influence of DEP on handling qualities (HQ) and how control laws and the architecture

of the control systems can take advantage of and improve the performance benefits brought up by DEP.

The aim pursued is the creation of an aerodynamic numerical code able to estimate the aerodynamic forces generated in the aircraft with propellers mounted in front of the wing in a DEP configuration, and to evaluate HQ and some performance characteristics through different methods, by the evaluation of the modes and the flight envelope when compared with a case where no blown is considered onto the wing.

The project's long-term goal is the proposition of a multidisciplinary design methodology that optimizes the possible HQ and performance characteristics through these DEP benefits. Thus, to proceed with a subsequent optimization process, and therefore to be able to quickly test several architectures and control strategies, the model should be kept in relative simplicity, with a low computation time and a certain flexibility, which allows the implementation and interfacing of several tools and new models and a quick mapping of the goal-selected variables chosen for the optimization.

2. Equations of flight

This section intends to explain the mathematical framework in which the author relies on the building of the model and the obtention of the HQ characteristics. First, equations of flights are shown, then the propulsion model is presented, and finally, it is explained how equilibrium in the equations is achieved.

2.1 General Equations and DEP particularities

The equations of flight are usually projected into the body system reference as the mass distribution of the aircraft around this frame is almost constant. This allows to take advantage of aircraft symmetry with respect to the plane $x_b - z_b$ which causes inertia crossed-products J_{xy} and J_{yz} to be equal to zero [7].

$$\begin{aligned}
-mg\sin\theta + F_{T_x} + F_{A_x} &= m(\dot{u} - rv + qw) \\
mg\cos\theta\sin\phi + F_{T_y} + F_{A_y} &= m(\dot{v} + ru - pw) \\
mg\cos\theta\cos\phi + F_{T_z} + F_{A_z} &= m(\dot{w} - qu + pv) \\
L_T + L_A &= I_x\dot{p} - J_{xz}\dot{r} + (I_z - I_y)qr - J_{xz}pq \\
M_T + M_A &= I_y\dot{q} + J_{xz}(p^2 - r^2) - (I_z - I_x)pr \\
N_T + N_A &= I_z\dot{r} - J_{xz}\dot{p} + J_{xz}qr - (I_x - I_y)pq
\end{aligned} \tag{1}$$

Being $(F_{A_x}, F_{A_y}, F_{A_z}, L_A, M_A, N_A)$ the aerodynamic forces and moments and $(F_{T_x}, F_{T_y}, F_{T_z}, L_T, M_T, N_T)$ the forces and moments due to propulsion. The angle of attack "α" and the side-slip angle "β", together with the aerodynamic airspeed "V" can be used for convenience:

$$\begin{aligned}
V &= \sqrt{u^2 + v^2 + w^2} \\
\beta &= \arcsin\frac{v}{V} \\
\alpha &= \arctan\frac{w}{u}
\end{aligned} \tag{2}$$

Regarding the aerodynamic forces and moments, in general, drag and lift coefficients are usually preferred, rather than C_X and C_Z, and can be easily obtained using the rotation matrix from the body to the aerodynamic frame matrix, as:

$$\begin{bmatrix} C_D \\ C_{Y_w} \\ C_L \end{bmatrix} = \frac{1}{\frac{1}{2}\rho V^2 S} \begin{bmatrix} cos\alpha\ cos\beta & sin\beta & sin\alpha\ cos\beta \\ -cos\alpha\ sin\beta & cos\beta & -sin\alpha\ sin\beta \\ -sin\alpha & 0 & cos\alpha \end{bmatrix} \begin{bmatrix} F_{A_x} \\ F_{A_y} \\ F_{A_z} \end{bmatrix} \tag{3}$$

These aerodynamic coefficients depend on the different flight variables, and usually, a linear-polynomial approximation is conventionally used, with some quadratic terms for the case of drag. A common hypothesis is to decouple the longitudinal dynamics and variables from the lateral ones. Assuming

these two hypothesis, for a conventional turbojet aircraft in an incompressible regime, the following is valid for longitudinal and lateral:

$$C_D, C_m, C_L = f(V, \alpha, \alpha^2, \hat{q}, \delta_e, \dot{\alpha}, \dot{\delta}_e) \tag{4}$$

$$C_Y, C_l, C_n = f(\beta, \hat{p}, \hat{r}, \delta_a, \delta_r, \dot{\delta}_a, \dot{\delta}_r) \tag{5}$$

Regarding forces and moments due to propulsion, F_{T_y} will always be zero, and L_T and N_T are zero always but for particular situations, such as an engine failure case. Calling C_T to the coefficient resulting from $C_T = \frac{1}{\frac{1}{2}\rho V^2 S} \| \overrightarrow{F_{T_x}} + \overrightarrow{F_{T_z}} \|$, this force will be the one acting also in C_{M_T}.
This whole development, however, will not be exact for a turbo-propeller aircraft. The presence of the propeller will create several aero-propulsive interactions between the propulsion system and the wing. In a DEP aircraft, this effect is desired for allowing for increased performance. In general, the effect will be more noticeable with respect to a twin turbo-propeller due to the higher number of engines and their adequate exploitation in terms of conception, configuration, and management to leverage in a beneficial way these aero-propulsive interactions.

Thus, in a DEP aircraft, the aerodynamic forces generated in the lifting surfaces of the wing are going to depend on the forces generated in the propellers at the front, due to the slipstream of the propeller created when generating thrust. By extension, the forces (and moments) generated in the horizontal wing are also going to be influenced. In an initial approach, and following once again a polynomial approximation, it is therefore valid to assume that the aerodynamic coefficients will also depend on some parameter directly related to the thrust, such as the thrust coefficient $C_T = \frac{T}{\frac{1}{2}\rho V^2 S}$, or the throttle lever position δ_x. When treating DEP aircraft, it will be more interesting to evaluate separately the effect of each engine on the different aerodynamic coefficients, in order to evaluate how their positioning in the wing influences the coefficients. Thus, the following will be valid in the longitudinal and lateral aerodynamic coefficients:

$$C_D, C_m, C_L = f(V, \alpha, \alpha^2, \hat{q}, \delta_e, \dot{\alpha}, \dot{\delta}_e, \delta_{x_1}, ..., \delta_{x_N}) \tag{6}$$

$$C_Y, C_l, C_n = f(\beta, \hat{p}, \hat{r}, \delta_a, \delta_r, \dot{\delta}_a, \dot{\delta}_r, \delta_{x_1}, ..., \delta_{x_N}) \tag{7}$$

It is important to say that, as a result of the interaction, new second-order coupling terms such as $\alpha\delta_x$ may have a non-negligible contribution.

2.2 Propulsion model

Propulsion with turbo-propellers presents some particularities with respect to conventional aircraft. This subsection will show how the modeling of thrust has been done. Propeller forces and thrust will have the form:

$$\begin{bmatrix} F_{T_x} \\ F_{T_y} \\ F_{T_z} \end{bmatrix} = \begin{bmatrix} \sum_{i=1}^{N_{eng}} T_i \cos i_p \\ 0 \\ \sum_{i=1}^{N_{eng}} T_i \sin i_p \end{bmatrix} \qquad \begin{bmatrix} L_T \\ M_T \\ N_T \end{bmatrix} = \begin{bmatrix} \sum_{i=1}^{N_{eng}} T_i \sin i_p y_i \\ \sum_{i=1}^{N_{eng}} (T_i \cos i_p z_i - T_i \sin i_p x_i) \\ \sum_{i=1}^{N_{eng}} -T_i \cos i_p y_i \end{bmatrix} \tag{8}$$

Being i_p the installation angle of the propeller. Terms L_T and N_T are equally zero in a conventional aircraft, but this is not the case in a DEP aircraft when flying with differential thrust. Regarding the coefficients due to thrust, the turbo-propellers thrust is strongly influenced by the inflow speed at the intake, especially at low speed. The speed at the intake of the propeller could be affected by the yaw speed "r" or by the side-slip angle "β", see [8]. Their effect is important as they influence the thrust coefficient of each engine and this effect will propagate to the lift and drag produced in the wing due to the differences in the slipstream generated behind each propeller. Due to this difference between the C_T of different engines, anti-symmetric roll or yaw moments could be generated.

$$V_{intake_i} = V \ \ cos\beta - r y_i \tag{9}$$

The model finally used for the thrust of each engine is the following, assuming that motors are electric and they do not suffer from rarefaction of air as turbomachines [9]:

$$T_i = \frac{P_E}{N_m} V_{intake_i}^{-1} \eta_m \eta_p \delta_{x_i} \tag{10}$$

As for gyroscopic effects, they are not considered as it is possible to cancel them with alternating fans and because in DEP small and light propellers are likely to be used to favour reaction time [10]. Finally, one of the known effects of propellers is that at an angle of attack they produce a force, parallel to the disk plane, and a moment. The force direction, normal or lateral, will depend on the angle between the disk and the flow, while the moment, in yaw or pitch, will depend on the direction of rotation [11][12][10]. These forces and moments will be neglected because of the expected low solidity of propellers and disc loading when distributing power across a larger propeller area [10]. As for the moment created by these normal forces, which are already small, propellers located at the wing leading edge generally have a level arm too small to impact the aircraft dynamics.

2.3 Static equilibrium

The aerodynamic forces evaluated in the aerodynamic tool and the propulsion forces are used in the general equations. In order to evaluate the different handling qualities and characteristics, an equilibrium for these equations has to be found.

The first two relations of the so-called inverse angular kinematic equations are added to the system of equations [1]:

$$\begin{aligned} \dot{\phi} &= p + (q\sin\phi + r\cos\phi)\tan\theta \\ \dot{\theta} &= q\cos\phi - r\sin\phi \end{aligned} \tag{11}$$

The set of equations is therefore $N_e = 8$. The variables are $[u, v, w, p, q, r, \theta, \phi]$ or also $[V, \alpha, \beta, p, q, r, \theta, \phi]$ after some transformations, so the number of variables is $N_v = 8$. The control surfaces deflections are $[\delta_a, \delta_e, \delta_R]$, which makes an amount of $N_u = 3$. Finally, if the thrust setting of the engines is included in the control vector $[\delta_{x_1}, ..., \delta_{x_i}, ..., \delta_{x_N}]$, there will be just an additional variable if differential thrust is not activated, or a number of additional variables equal to the number of engines "N_m", if it is. This makes a total amount of unknowns of $N_v + N_u + 1 = 12$ with no differential thrust, or $N_v + N_u + N_m = 11 + N_m$ with it, so the problem is over-determined anyway. For being able to solve the problem, the number of equations plus the number of constraints must equal the number of variables to determine. Usually 4 variables are fixed (so 4 constraints are introduced) and there is a unique solution for equilibrium. These parameters are normally $[V, \beta, \gamma, \Omega]$, able to fix the flight condition. The new variables γ (the flight path angle) and Ω (the turn rate) have been introduced but they have also their own two new equations, so the equilibrium between equations and variables is respected:

$$\sin\gamma = \cos\alpha\cos\beta\sin\theta - \sin\beta\sin\phi\cos\theta - \sin\alpha\cos\beta\cos\phi\cos\theta \tag{12}$$

$$\Omega = (q\sin\phi + r\cos\phi)\frac{1}{cos\theta} \tag{13}$$

However, if differential thrust is considered, then the thrust setting of each engine is different and the problem is over-determined even when fixing 4 parameters. The problem becomes therefore a problem of optimization of an objective- function under constraints. The objective function to minimize can vary depending on the results desired, but the power required for maintaining equilibrium is a good function for a general optimization and makes sense under the idea of minimizing the power to install on the aircraft. Finally, for an optimization process, it is required to set higher and lower bounds on the control inputs and variables that depend on the flight phase and the aircraft.

3. Aerodynamic database

This section will explain which are the different aircraft and aerodynamic models used for the construction of a code able to predict the aerodynamic forces when the different interactions brought by DEP are considered.

3.1 Reference Aircraft

Commuter-regional aircraft are the best candidates for a future-general implementation of electric propulsion and consequently for leading the first generation of DEP aircraft. Therefore, they are the best option for studying and showing the effects of this kind of propulsion. Following this guideline, two aircraft have been chosen for the simulations. The first one is an ATR 72 [13], [14] used as a general reference model due to its good representation of a subsonic commuter, turbo-propelled aircraft. The second one is the Radio-controlled model DECOL. DECOL is a low-speed DEP demonstrator which has been designed and built at ISAE-Supaero. DECOL is useful as an experimental platform to test the performance of this kind of propulsion and for the comparison of numerical results and tendencies. In order to avoid repetition of results, as the model and methods used have been the same for both aircraft, only results for the ATR are shown in this paper. Results from DECOL will be however used in the future in order to compare them with flight campaigns to be done. General characteristics of the ATR are shown in table 1.

Characteristics	Values
Wingspan	27.05 m
Wing surface	61 m^2
Overall Length	27.17 m
Mass	21500 Kg
Mean aerodynamic chord	2.303
Ref. cruise speed	510 m/s
Total available power	4000 KW
Horizontal Tailplane area	11.13 m^2
Vertical Tailplane area	12.5 m^2

Table 1 – ATR 72 general characteristics

In order to properly analyze the performances and qualities of DEP aircraft, it is important to set a fair baseline from which to compare them and their conventional versions. This is the reason why no change has been introduced in terms of mass, geometry or available power for the ATR 72 between its regular configuration and the DEP one. The only parameter varied has been the number of engines, while a conventional ATR 72 has two engines, the version studied here has 12.

3.2 Aerodynamic coefficients and forces

A brief introduction to the different aerodynamic interactions when considering DEP will be presented, explaining why some of them have been considered and how, through different models, and why some have been neglected as they were considered not important for the study and understanding of HQ.

When considering an aircraft with DEP, several aerodynamic differences will appear due to the presence of the turbo-propellers and their interactions with the other elements. The propellers will generate their own aerodynamic forces and moments, will interact between them, or will interact with the rest of the aircraft through the slipstream. The slipstream is the region behind the propeller resulting from the deflection of the stream tube of flow after passing through it. This region is characterized by a velocity of the axial flow higher than the undisturbed flow velocity and by the presence of a rotational velocity.

Propeller-Wing

There are two main effects of the propeller slipstream in the wing, due to the configuration of the resultant field of velocities. Although this field is complex, there are two major components, an axial one, along the propeller's rotational axis, and a tangential one called swirl.

The axial velocity will lead to an increase in dynamic pressure through the increase of the velocity of the portions of the wing immersed in the slipstream. There will also be a change in the total angle of attack. This increase in local free-stream velocity produces an increase in lift and can lead to delayed stall through increases in the local section Reynolds numbers. The presence of the slipstream will also increase the efficiency of the flaps, and will generate an increased tail-off pitching moment in a nose-down sense.

On the other hand, swirl increases the local angle of attack after the upwards moving half of the propeller and decreases it in the other half. The wing after the propeller is however known to act as a stator vane, reducing the effective swirl and contributing to the generation of thrust, a phenomenon known as swirl recovery. Swirl has been neglected as it's a secondary effect with respect to the increase in dynamic pressure and because effects on the lift of one side of the disk can be assumed to be countered by the effects on the other side. The schematic impact of propeller-blowing on a wing is shown in figure 1.

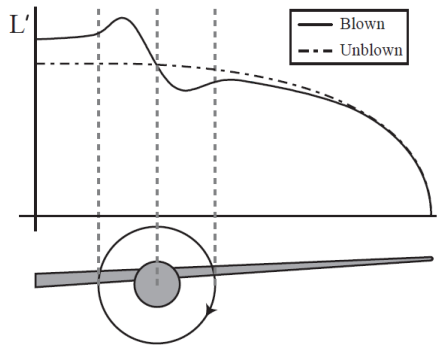

Figure 1 – Generic lift distribution of a blown and unblown wing, from reference [15]

The propeller-wing interaction is a two ways interaction as the wing can also influence the propeller. Since the wing circulation tends to generate upwash upstream of the wing, the propeller disk will encounter non-uniform flowfields that will decrease its performance [1]. The perturbation will vary depending on the distance between the propeller and the wing. In this setup propellers are sufficiently far from the wing (around one radius of the disk) to consider this effect negligible.

Propeller-propeller

Propellers, when considering a DEP configuration, may interact with the adjacent propellers, modifying the field of velocities in a forward flight. The interaction between propellers in a DEP configuration has shown to slightly reduce the performance of the engine and its thrust [16]. Moreover, the interaction between propellers does not appreciably modify the streamwise development of the slipstream. Hence, this reduction has been considered not to be relevant for an HQ analysis in an early conception design.

Propeller-horizontal tail

The slipstream will also interact with the horizontal tail through two mechanisms of interference: the increased downwash and the higher dynamic pressure in the slipstream. As a result of the increased lift in the wing, downwash will be increased. This effect will not occur just in the slipstream tube, but in the whole flow field, and will affect the tail reducing its contribution to longitudinal stability [17]. The increased dynamic pressure in the slipstream will cause the part of the tail immersed in the slipstream to experience a higher average dynamic pressure, increasing its effective C_{L_α}. Whether the tail is actually in the slipstream depends on many parameters, such as its vertical position, the angle of attack, the flap deflection, or the power setting [17].

Propeller-Vertical tail

Propeller slipstream also affects the vertical tail and therefore the directional stability and control of the aircraft. The engine whose blade goes up next to the fuselage is known to produce a stronger crossflow due to the distribution of the swirl and the resulting trailing vortex [17]. In the case of co-rotating propellers, if the engine whose blade goes down near the fuselage fails, the cross-flow of the other on the vertical tail will create a strong yaw moment in addition to the one of the engine not being compensated by the engine who failed. This is why the down-blade engine near the fuselage is called "critical engine". While these effects have to be considered for the vertical tail sizing, this special case of engine failure will not be considered here and so this effect is not taken into account.

3.3 Model construction

Several methods exist for the building of the aerodynamic database when considering unconventional configurations. Methods can be divided into analytical, empirical or semi-empirical, and numerical. Traditional analytical and empirical or semi-empirical methods are not adequate for unconventional configurations as they are developed on a database of conventional aircraft. Regarding the numerical methods, their complexity can vary from a simple Vortex-Lattice method (VLM) with a time computation in the order of seconds, to a complete CFD analysis with huge time and computation costs. For a preliminary design, and as this study is intended to be followed by an optimization process, a mix of different simple-numerical methods and DEP-based surrogate models have been used. These models capture the different possible effects which were considered to be the most important for the study of the distributed propulsion interactions. A previous model developed in the frame of this project is used as a baseline for the study. The model uses a combination and interfacing of simple tools and, taking advantage of its flexibility, it has been extended through modifications and the implementation of new surrogate models from the literature.

3.3.1 Existing model

First, a VLM method from the open-source tool OpenVSP [18] is used to retrieve all the aerodynamic coefficients for a version of the aircraft without the vertical tail. Some of these coefficients will be later modified. The contribution of the fuselage and wing to the majority of lateral coefficients has been found to be adequately estimated by the VLM.

For the calculus of the vertical tail-related coefficients, a semi-empirical method, presented by Nicolosi [19], called VeDSC, has been used. The model has been developed through numerical CFD computations complemented with wind tunnel tests. It assumes a decoupling of lateral coefficients into fuselage, wing, and vertical tail contributions and it introduces a redefinition of the vertical tail lift slope through corrective coefficients. More information can be found in [19]. The contribution of the vertical tail to derivatives $C_{Y_\beta}, C_{l_\beta}, C_{n_\beta}, C_{Y_p}, C_{l_p}, C_{n_p}, C_{Y_r}, C_{l_r}, C_{n_r}$ is calculated through this method, and also the complete derivatives $C_{Y_{\delta_r}}, C_{l_{\delta_r}}, C_{n_{\delta_r}}$ whose whole contribution comes from the tail. All these derivatives suffer therefore variations with respect to OpenVSP calculus.

For the wing, it is divided into a sufficiently-high number of slices (wingspan stations, noted "j") and the C_{L_j} coefficients are extracted. For the calculus of $C_{L_{0,j}}$ of each slice, two angles of attack are used. In order to model the increase in the dynamic pressure of the wing and the change in the angle of attack after the propeller of each station, the model proposed by Patterson [1] is used. In this model, the speed after the propeller is calculated through momentum theory [20], and a surrogate model based on CFD simulations is used for the calculus of "augmented" lift coefficients, using a multiplier L_{m_j} for each station. The parameters used for creating the surrogate model are the augmented speed, the size of the actuator disk, and the distance between the actuator disk and the wing leading edge, dimensioned with the freestream speed and the chord respectively. The method is developed in 2d and generalized to 3d using a pre-existing lift distribution and assuming linear propagation. Further can be found on [1]. A scheme can be seen in figure 2.

Regarding the drag in the wing, there are several contributions to take into account. For the unblown friction drag, the results from the VLM are used. The increase in the friction drag due to the increase

in the local velocity, either because of the slipstream in the sections behind the propeller or because of the presence of yaw speed, has been added later. As this friction depends on the development of the boundary layer and the propeller is known to force the transition earlier, as observed in [21], [22], to simplify the problem the transition from laminar to turbulent is forced at 10% of the chord for the ATR [11]. Finally, for the calculus of the induced drag, the lifting line theory is used, and the contributions due to the deflection of local speed after the propeller or because of the presence of roll speed modifying the angle of attack have been also considered. The pressure drag has only been calculated for the stall as it is considered of less importance in slim bodies for a normal regime of angles of attack. For a detailed explanation of the previous model, the reader is referred to [10].

3.3.2 Model extension

The original model has been augmented in order to capture the possible influence of lateral and longitudinal flight variables on the existing interactions in order to estimate the lateral and longitudinal stability and HQ characteristics. For each wingspan station, the effects of yaw, roll speed, and side-slip angle have been taken into account in the speed and the angle of attack seen by each section, similar to what happens with the intake speed of the engines, as explained in section 2.2. For the angle of attack, modification is $\Delta\alpha = \frac{py}{V_\infty}$. In order to obtain the yaw and roll moments, integration along the wingspan is effectuated, so the wing contribution to derivatives Cn_p and Cl_p is recalculated over the VLM. The effects of these variables are introduced and later let to propagate into the model. The model has been augmented for accounting for flaps and ailerons, by assuming that these two modify the zero lift line of the airfoil [23]. This modification is introduced into the zero lift angle and is propagated in the model.

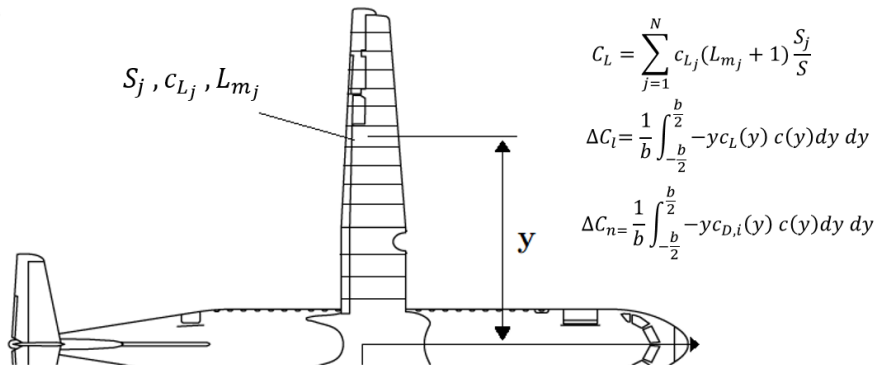

Figure 2 – Model methodology

Regarding the terms affecting the longitudinal stability, a method for the determination of slipstream effects from Obert [24], [25] has been used. The method is based on momentum theory and combined with a correlation of wind tunnel data. The method is used for evaluating:

- The change in tail-off pitching moment, with flaps retracted and deflected.
- The slipstream position with respect to the horizontal tail, to measure the effects on the average dynamic pressure and the wet area.
- The change in the average downwash angle due to the slipstream effect, which affects the horizontal tail and subsequently the lift generated here and the pitching moment affectation.

Finally, a characteristic of blowing is the delay in the appearance of the stall. The stall model is based on Jameson [23]. Numerical 2D simulations are run for manually fixing the stall limit and for evaluating the airfoil pressure drag. The Patterson-modified angle of attack is used to determine if a wing section is stalled. The main idea is not to give a correct evaluation but to model the delay in the stall and avoid equilibrium beyond the stall with the trim algorithm.

The current model presents some advantages over a more complex one. For instance:

- The model is flexible to the number of engines and their position. By neglecting the propeller-propeller interaction, the effects of the engines on the wing are considered locally and any change in their number or position is quickly and independently computed for evaluation of lift, induced and friction drag, and roll and yaw, without recalculating the aerodynamic database.
- The computation time is kept very low, the aerodynamic tool can compute the forces for a high number of calls within seconds.
- The model uses inputs from different tools and is prepared for interfacing with other preliminary aerodynamics evaluation tools, for eventually considering more interactions with an easy implementation.

Table 2 shows a summary of the different modeled interactions resulting from DEP and of the methods used to characterize them, while figure 3 is a flow chart showing how the tool has been organized and how it works.

Table 2 – Methods of characterization

Component/Feature	**Modeling**
Wing, tail	VLM (OpenVSP)
Bluff bodies	VLM (OpenVSP)
Propeller thrust	Momentum theory
Propeller normal/side force	Neglected
Propeller moments	Eng. method
Effects of propellers on wing	Patterson [1]
Effects of propellers on tail	Obert [24]
Propeller-propeller interaction	Neglected
Airframe - propellers interaction	Neglected

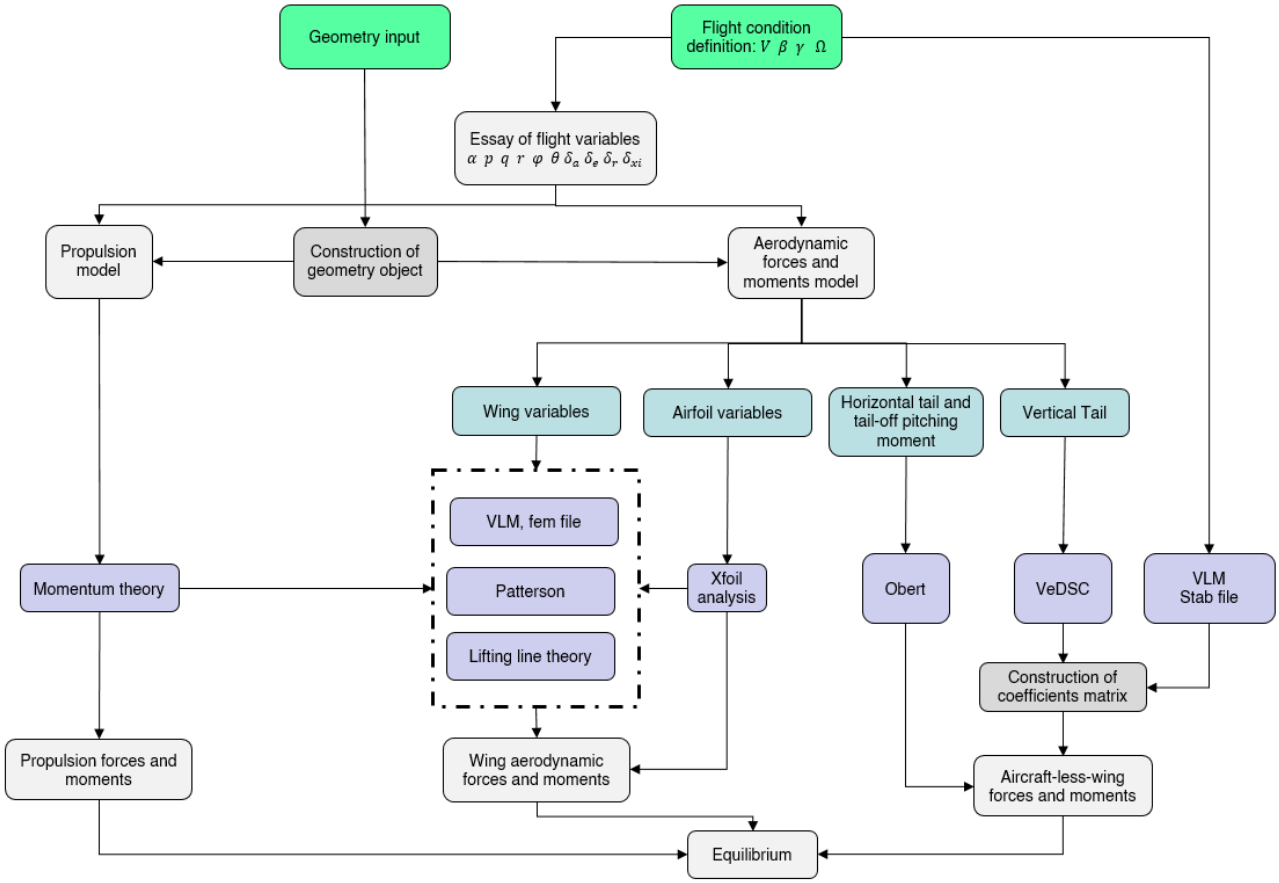

Figure 3 – Model flowchart

4. Results

Once a model is implemented, it is possible to evaluate some performance characteristics and HQ through several criteria. Some of these are the evaluation of the different longitudinal and lateral-directional modes, the evaluation of the aerodynamic coefficients when the slipstream effect is considered, or the construction of a flight envelope.

4.1 Aerodynamic coefficients

This subsection will explain how the different aerodynamic coefficients have been obtained and what are the main changes regarding their dependencies when compared with a conventional aircraft where no propeller-wing interaction is considered.

In order to do this, first, the aircraft is trimmed at a given point, as shown in table 3. This point has been chosen as it is representative of a low-speed cruise at low altitude, for example on a stage near the approach to the runway. At low velocity, the speed past the propellers and the thrust generated are higher, and the same accounts for the thrust coefficient C_T, which leads to a higher importance of the interaction between the wing and the propellers.

Table 3 – Trim point at low-speed cruise

Speed [m/s]	α (°)	δ_e (°)	δ_x[%]
72	5.57	-5.34	31,5

For obtaining the aerodynamic coefficients, two methods are used. The second represents advantages over the first as it allows to obtain coupled aerodynamic coefficients, but the first one can be opportunely used to study some tendencies.

In the first method, the different flight variables of the problem are varied, one by one, around the mentioned cruise trimmed point, while keeping the rest at their trim value. The aerodynamic forces are calculated for each variation. Later, one-dimension splines are used for the curve approximation and derived at the trimmed point to obtain the aerodynamic coefficients at that point. These coefficients depend therefore on just one variable and are valid around the trim point.

In the second method, a polynomial approximation is done using orthogonal least-squares. Different bounds are selected around the trimmed values of the flight variables. After that, a systematic sample is generated and an optimization tool for polynomial approximation developed in ONERA, (APRICOT, [26]) is used to obtain the different coefficients as polynomial expressions. As a result, the coefficients obtained can depend on several coupled variables or show non-linear behaviours. For the longitudinal variables, the throttle lever of all the engines has been varied in unison, in order to keep the aircraft in a longitudinal case, while for the lateral-directional variables the throttle lever has been varied alternatively for the engines of each semi-wing.

The results from the least-squares method show the strong influence of the propeller-wing interaction on the general aerodynamic coefficients. The propellers, aside from creating forces and moments purely due to thrust, modify the aerodynamic forces and moments (and hence the coefficients) noticeably. Therefore derivatives with respect to the thrust setting δ_x are not null and new terms appear depending on it, alone or coupled with others.

Regarding the longitudinal case, the interaction produces the appearance of coefficients that depend on δ_x: $C_{L_{\delta_x}}, C_{D_{\delta_x}}$ and $C_{m_{\delta_x}}$, and of the couple δ_x, α: $C_{L_{\alpha,\delta_x}}, C_{D_{\alpha,\delta_x}}$ and $C_{m_{\alpha,\delta_x}}$. The general structure of the coefficients can be seen in equation 14. Dependencies on the dimensionless speed $\hat{V}$ can eventually be simplified for a better comprehension of results as they are the less important ones, varying the global relative error between around 1% and 8% when including them or not.

$$
\begin{aligned}
CL &= C_{L_0} + C_L(\hat{V}, \alpha, \hat{q}, \delta_e, \delta_x, \alpha\hat{V}, \delta_x\hat{V}, \alpha\delta_x) \approx C_L + C_L(\alpha, \hat{q}, \delta_e, \delta_x, \alpha\delta_x) \\
C_D &= C_{D_0} + C_D(\alpha, \alpha^2, \hat{q}, \delta_x, \delta_e, \alpha\delta_x, \delta_x\hat{V}, \delta_x\hat{V}^2, \alpha\delta_x\hat{V}) \\
C_m &= C_{m_0} + C_m(\alpha, \alpha^2, \hat{q}, \delta_e, \delta_x, \alpha\delta_x)
\end{aligned} \tag{14}
$$

Comparison of results between coefficients obtained with one-dimension splines and the ones obtained with least-squares is interesting to check on the polynomial approximation and to compare between the case where the interaction is considered and the clean configuration. Results show how the derivative of the lift coefficient with respect to the angle of attack for a given throttle lever in the case of interaction, is equal to the one where there is no interaction considered plus a term depending on the angle of attack and the throttle lever. Mathematically this is expressed as:

$$
\frac{dC_L}{d\alpha}^{Int}_{\delta_x=\delta_{x_0}} = \frac{dC_L}{d\alpha}^{No\ Int} + C_{L_{\alpha,\delta_x}}\delta_{x_0} = C_{L_\alpha} + C_{L_{\alpha,\delta_x}}\delta_{x_0} \tag{15}
$$

Table 4 – Thrust-angle of attack influence on lift coefficient

$\frac{dC_L}{d\alpha}^{Int}_{\delta_x=0.315}$	$\frac{dC_L}{d\alpha}^{No\ Int}$	$C_{L_{\alpha,\delta_x}}$
6.0321	5.7225	0.9157

With terms $\frac{dC_L}{d\alpha}^{Int}_{\delta_x=\delta_{x_0}}$ and $\frac{dC_L}{d\alpha}^{No\ Int}$ having been obtained through the one-dimension splines method and $C_{L_{\alpha,\delta_x}}$ with the orthogonal least-squares method. Values for the case of equilibrium in table 3 are shown in table 4. This behaviour is shown for the lift and drag coefficients in figures 4 and 5. For the lift, the behaviour is almost linear in α but for the drag, the quadratic term is slightly appreciated.

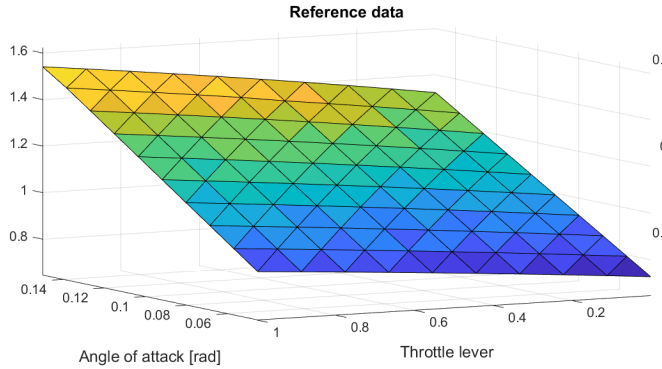

Figure 4 – C_L as a function of α and δ_x

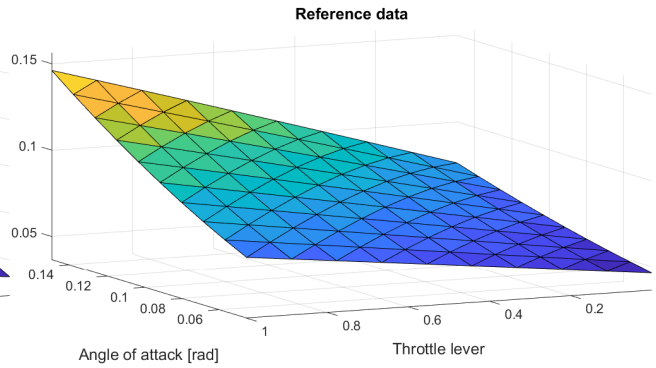

Figure 5 – C_D as a function of α and δ_x

Regarding the lateral case, there is a new term depending on the thrust setting, but there are no coupled coefficients this time.

$$
C_Y, C_l, C_n = f(\hat{p}, \hat{r}, \delta_a, \delta_r, \beta, \delta_x) \tag{16}
$$

It is interesting here, to look at what is brought when using the one-dimension splines and calculating the derivative of the coefficients of lift, roll moment, drag and yaw moment, C_L, C_l, C_D, and C_n, with respect to the thrust level of each engine, for instance:

$$
C_{L_{\delta_{x_1}}}, C_{l_{\delta_{x_1}}}, C_{D_{\delta_{x_1}}}, C_{n_{\delta_{x_1}}}, ..., C_{L_{\delta_{x_i}}}, C_{l_{\delta_{x_i}}}, C_{D_{\delta_{x_i}}}, C_{n_{\delta_{x_i}}}, ..., C_{L_{\delta_{x_N}}}, C_{l_{\delta_{x_N}}}, C_{D_{\delta_{x_N}}}, C_{n_{\delta_{x_N}}} \tag{17}
$$

The results are plotted in figure 6 and shown in table 5. For the figure, the horizontal axis represents the engines (from 1 to 12), being the number one the engine at the left wing tip, and the number twelve the engine at the right wing tip. For the table results are just shown for one semi-wing, being lift and drag coefficients symmetric and roll and yaw moment ones anti-symmetric for the other semi-wing.

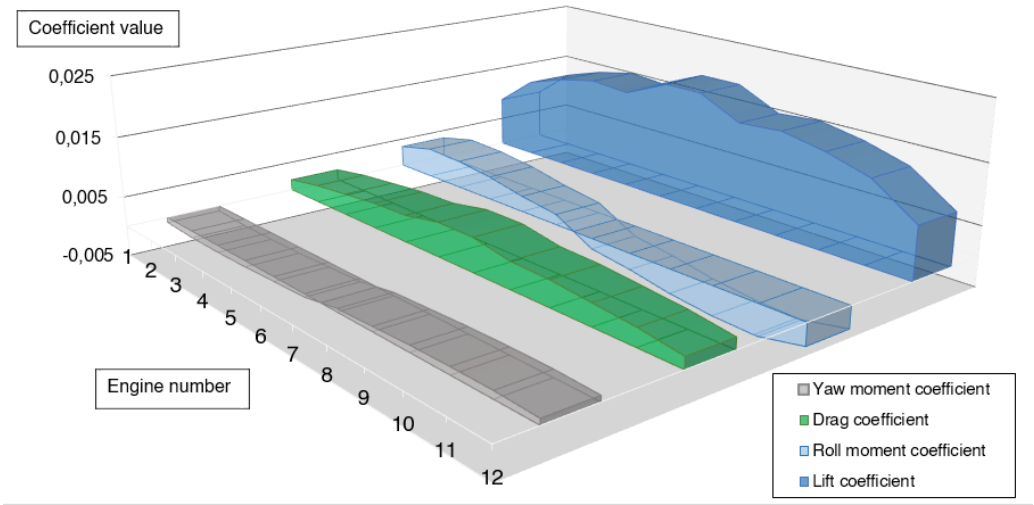

Figure 6 – Aerodynamic coefficients of each engine

As expected, when varying their throttle lever, inner engines are more efficient for producing lift than the outer ones. This is due to the higher lift present in the inner part of the wing in the clean configuration. For the torque moments, there is a trade-off between this factor and the lever arm to the symmetric plane of the aircraft (where the center of gravity is located). Results show that engines at the tip are not the ones able to generate more aerodynamic moment, even though they have the largest lever arm, due to the reduced lift produced at the wing tip, but the ones next to them. Evidently, this changes when taking into account also the moment due to thrust.

Table 5 – Aerodynamic coefficients of each engine

	$/\,\partial\delta_{x_1}$	$/\,\partial\delta_{x_2}$	$/\,\partial\delta_{x_3}$	$/\,\partial\delta_{x_4}$	$/\,\partial\delta_{x_5}$	$/\,\partial\delta_{x_6}$
∂C_L	0.00876	0.01376	0.01587	0.01723	0.01672	0.01998
∂C_l	0.00358	0.00502	0.00473	0.00394	0.00266	0.00175
∂C_D	0.00184	0.00289	0.00355	0.0042	0.00443	0.00562
∂C_n	-0.0009	-0.00118	-0.00118	-0.00106	-0.00078	-0.00052

4.2 Flight Envelope

Due to the extra lift generated when the flow is accelerated in the slipstream, one of the advantages of mounting propellers in front of the wing is the possibility to fly at lower speeds, with respect to a configuration where DEP is not used. Therefore these in-front-of-the-wing propellers can be seen as a sort of hyper-lifting device, able to reduce the stall speed.

For this section, the optimizer was adapted. The problem is now described. The flight is considered to be a symmetric, horizontal rectilinear flight, with no bank angle, which allows to make null all the lateral variables ($\beta, p, r, \phi, \delta_a, \delta_R = 0$) and also also the pitch rate and the flight path angle, ($q = \gamma = 0$). Finally, no differential thrust is considered, this is, the thrust setting for all the engines is selected to be equal and therefore the thrust given by them is the same. Instead of writing the throttle lever of each engine as $[\delta_{x_1}, ..., \delta_{x_N}]$, just the notation δ_x is used to refer to the thrust setting of all of them. The state vector with 5 variables is:

$$x = [V, \alpha, \theta, \delta_e, \delta_x] \tag{18}$$

The equations used are the first, third, and fifth of system 1, and the first of system 12, with previous simplifications.

$$\begin{aligned} 0 &= -mg\sin\theta + F_{T_x}(\delta_x) + F_{A_x}(\alpha, \delta_e, \delta_x) \\ 0 &= mg\cos\theta + F_{T_z}(\delta_x) + F_{A_z}(\alpha, \delta_e, \delta_x) \\ 0 &= M_T(\delta_x) + M_A(\alpha, \delta_e, \delta_x) \\ 0 &= \alpha + \gamma - \theta \end{aligned} \tag{19}$$

To note that 6 variables are present in these four equations: $(V, \alpha, \theta, \delta_e, \delta_x, \gamma)$ but there exists also the constraint $\gamma = 0 \leftrightarrow \theta = \alpha$, so the problem is oversized by one. Higher and lower bounds are added to the control inputs due to the physical limitations. For the speed and the angle of attack (or the pitch angle), indicative limits have been set, although as explained there is a stall model for the interaction case that could mark the limit in this optimization.

Table 6 – Variables bounds

Variable	Bound
$V \ [m/s]$	$20 < V < 100$
$\alpha \ (^\circ)$	$-5 < \alpha < 25$
$\delta_e \ (^\circ)$	$-23 < \delta_e < 13$
$\delta_x \ (\%)$	$0 < \delta_x < 100$

Finally, the objective function is the aircraft velocity, given adequately so that the minimization algorithm can calculate a proper Jacobean matrix.

$$f_{obj} = V = \sqrt{\frac{mg - F_{T_Z}\cos\theta - F_{T_X}\sin\theta}{\frac{1}{2}\rho S\, C_L(V, \alpha, \delta_e, \delta_x)}} \tag{20}$$

Four cases are studied for the ATR 72. In the first case, the propeller-wing interaction is considered, using the model previously explained, with no flaps deployed. In the second, third, and fourth cases the aircraft is considered without the interaction, so the aerodynamic model is entirely based on the VLM, with no flaps deployed, flaps to 15°, and flaps to 30° respectively.

Results for the four cases are shown in table 7 and figure 7. The case with the interaction shows an effective lower stall speed, with a reduction of almost 4.5 m/s (16 km/h) when compared with a clean configuration, similar to the one achieved in the case without interaction when deflecting the flaps to 15°. Due to the slipstream, more lift is produced and this allows to fly at a lower speed given the same angle of attack. The slipstream effect creates however a strong nose-down pitching moment,

that obligates to deflect the elevator to its inferior limit (-23°) to counter this effect. Hence, is the detachment in the elevator the one creating the stall, instead of the one in the wing, being the angle of attack at this point (14.67°) inferior to the one set for the stall (17.3°). The angle of attack from case 1 (14.67°) is set as the upper bound for the non-interaction cases (2, 3, and 4), as there is not a stall model for these cases and consequently the optimizer could reach the indicative limit set in table 6, which is highly unrealistic. In addition to allowing for a better comparison of results, it shall be remarked that the presence of the slipstream leads to a later detachment of the boundary layer, so the stall is likely to occur for higher angles of attack, so this proceeding seems coherent.

Table 7 – Minimum-speed equilibrium at sea level

Case	Speed [m/s]	α (°)	δ_e (°)	δ_x[%]
Interaction, not flaps deflected (1)	49.75	14.67	-23	56.7
Not interaction, not flaps deflected (2)	54.228	14.67	-11.99	28.4
Not interaction, flaps to 15° (3)	48.18	14.67	-12.74	28.5
Not interaction, flaps to 30° (4)	44.87	14.67	-13.31	28.8

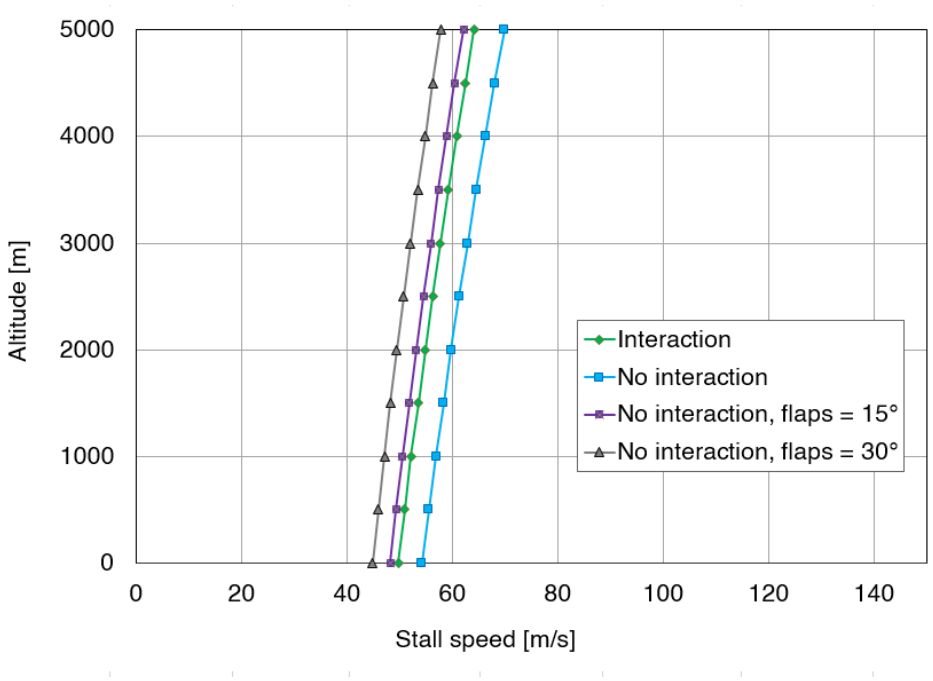

Figure 7 – Flight envelope

For case 1, the lift and drag distributions are plotted in figures 8 and 9. The C_D plotted accounts for the induced drag (C_{D_i}), the drag coming from lift due to deflection of the slipstream (C_{D_w}), and the increase in the friction drag due to the augmented speed in the slipstream (C_{D_0}). It would still be necessary to add the clean-friction drag coefficient of the aircraft, obtained with VLM.

The equilibrium of the two longitudinal control variables δ_e, δ_x, and of the angle of attack α, can be seen in figure 10 for a low altitude-sea level, comparing the blown and unblown cases. Although there may be an over-estimation of the drag, as commented, to achieve the minimum speed, a higher thrust setting is required for the blown case, but lower angles of attack are possible. Above the minimum speed, there exists the typical minimum for the required thrust and after it, the thrust required grows again until the maximum where the maximum speed is given.

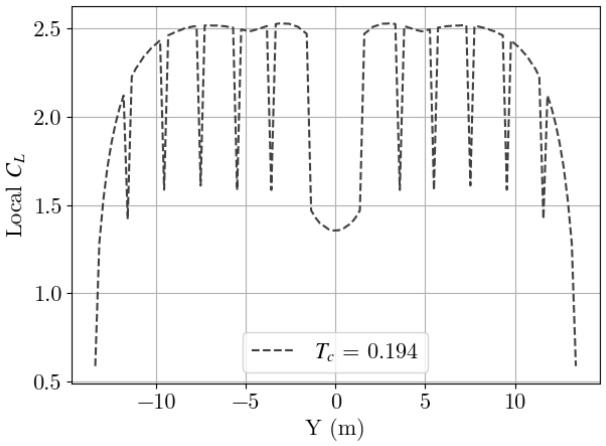

Figure 8 – CL distribution, case 1

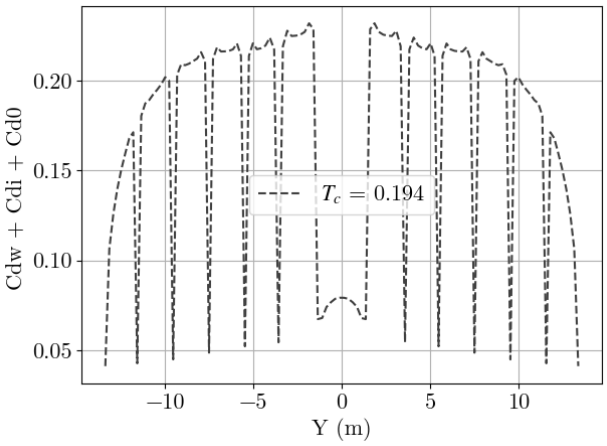

Figure 9 – CD distribution, case 1

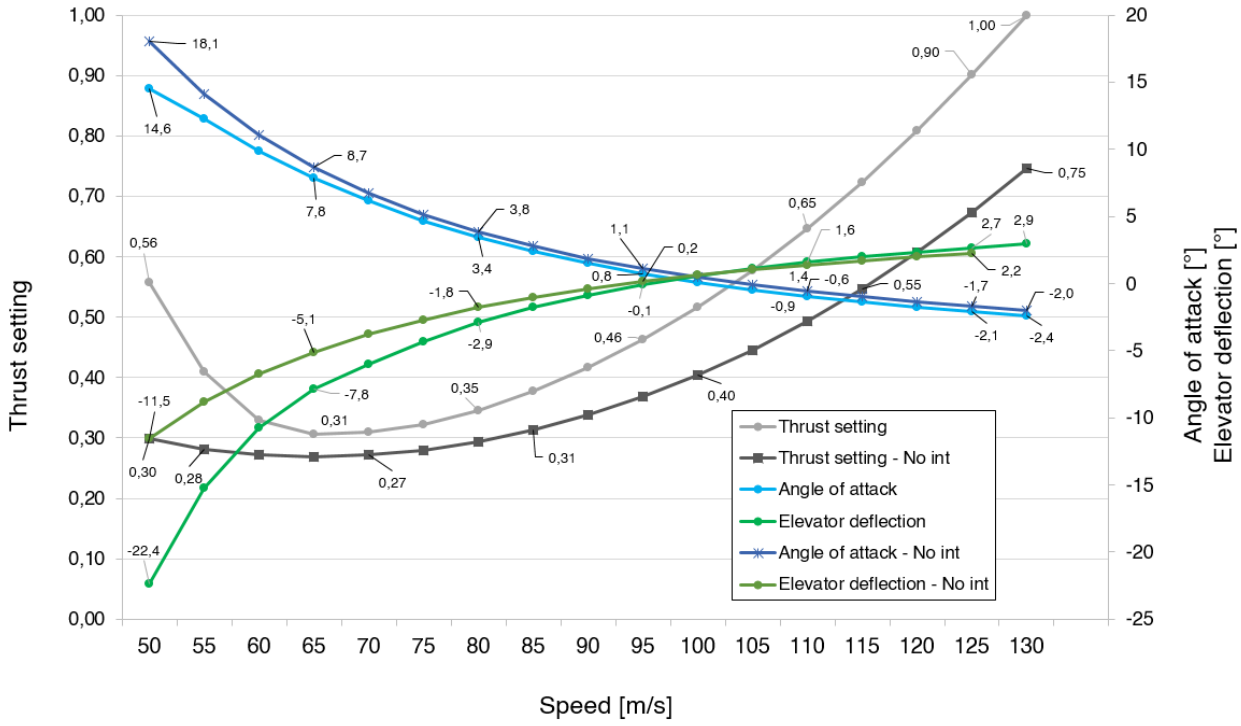

Figure 10 – Equilibrium values at low altitude for cases 1 and 2

In summary, when considering the interaction, the process of trying to fly at lower speeds leads to higher thrusts and speeds after the propeller, and therefore to high deflections of the stream past the propeller's disks. This effect creates augmented lift but the payback is that there exists also a very noticeable increase in the drag, particularly in the induced drag and the "wet" drag, that considers the deflection of the stream after the propeller. Essentially, a part of the thrust is being used for generating more lift but the new lift itself creates more drag, which obligates to set a high thrust setting. Propellers are therefore working here as a hyper-lifting device. The situation with both flaps at 30° and interaction is not plotted as the drag generated is so big that the engines are forced to work in full regime and the aircraft is forced to fly with a low angle of attack in order not to generate more drag, being the reduction of the speed with respect to the case without flaps very small.

4.3 Handling qualities assessment

Finally, the flight modes of the aircraft are calculated. When calculating the different modes and comparing them between the case with interaction and the case without it, no remarkable differences were observed. The largest difference occurs for the roll subsidence mode which happens to be faster when considering the interaction, but the difference is not considered relevant enough to show it. Still, the biggest influences on the modes are proven to be the airspeed and the location of the center of gravity and, so, the analysis here studies their influence on the different modes for the interaction case. In order to obtain the flight modes, the system from equations 1 and 11 are linearized around several flight conditions, for instance, in equilibriums where the state vector accomplishes $\dot{x} = 0$, $(x = [V, \alpha, \beta, p, q, r, \phi, \theta])$ and the linear state space representation is obtained:

$$\begin{aligned} \dot{x} &= Ax + Bu \\ y &= Cx + Du \end{aligned} \tag{21}$$

The eigenvalues of matrix A are plotted in figures 11 and 12. They have been obtained for three different airspeeds (70, 80, and 90 m/s) and for 6 different positions of the center of gravity (when measured from the tip of the aircraft: 11.25, 11.75, 12, 12.25, 12.75, and 13.25 m), always at low altitude - sea level. As typically expected, the phugoid (PHG) mode shows to be a very badly damped oscillatory mode and does not change when varying the center of gravity, depending only on the airspeed. Regarding the short period oscillation mode (SPO), there is a small influence of the airspeed, but it shows to depend mainly on the position of the center of gravity, as in a classical aircraft. When the center of gravity is shifted afterwards (AFT CG), the two complex poles first approach the real axis through the same vertical line (they have the same real part) and then they became two real poles, moving through the real axis, one of them towards the right and crossing the positive plane when the center of gravity arrives at the neutral point of the aircraft, becoming, therefore, an unstable oscillation, and the other towards the left, becoming more negative.

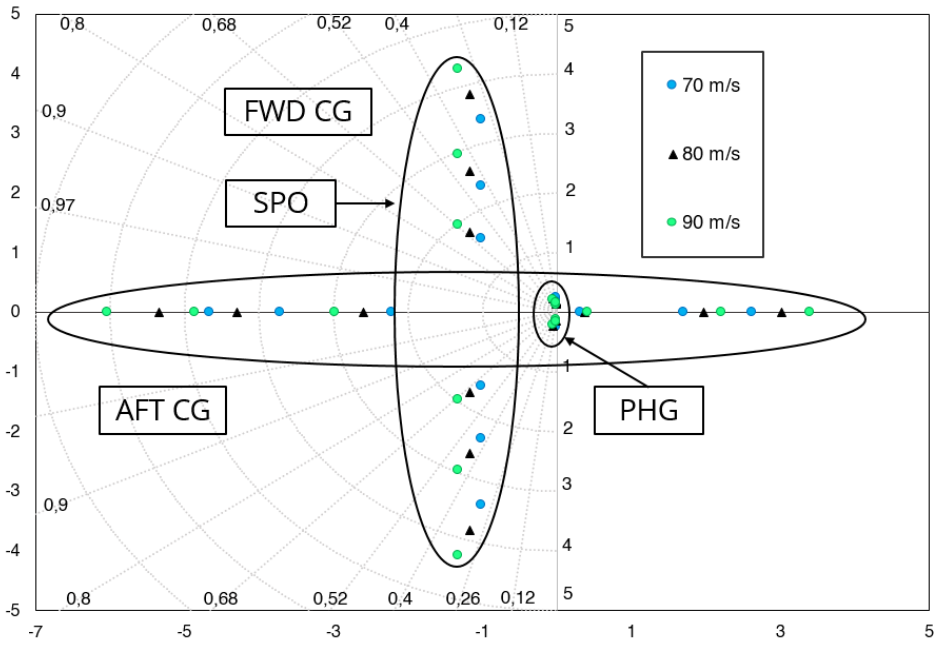

Figure 11 – Longitudinal modes

Regarding the roll subsidence and the spiral mode, as typically, they are both aperiodic, being the roll mode fast and the spiral extremely slow. They both show small dependency with the center of gravity position and a more noticeable dependency with the airspeed. The spiral mode shows to be very near to the origin, positive (and unstable, therefore), but extremely slow, and becomes negative (but once again it is almost imperceptible) when increasing speed or when shifting a lot the center of gravity

backwards. As expected, the Dutch roll mode is badly damped and shows slightly more influence on the center of gravity than the other two lateral modes. If the center of gravity is moved afterwards, due to the modification in C_{n_β}, the Dutch roll will approach the origin while keeping an oscillatory form, and will eventually cross to the positive region of the real-imaginary plane, becoming unstable. However, the center of gravity has to be extremely shifted backwards to achieve this.

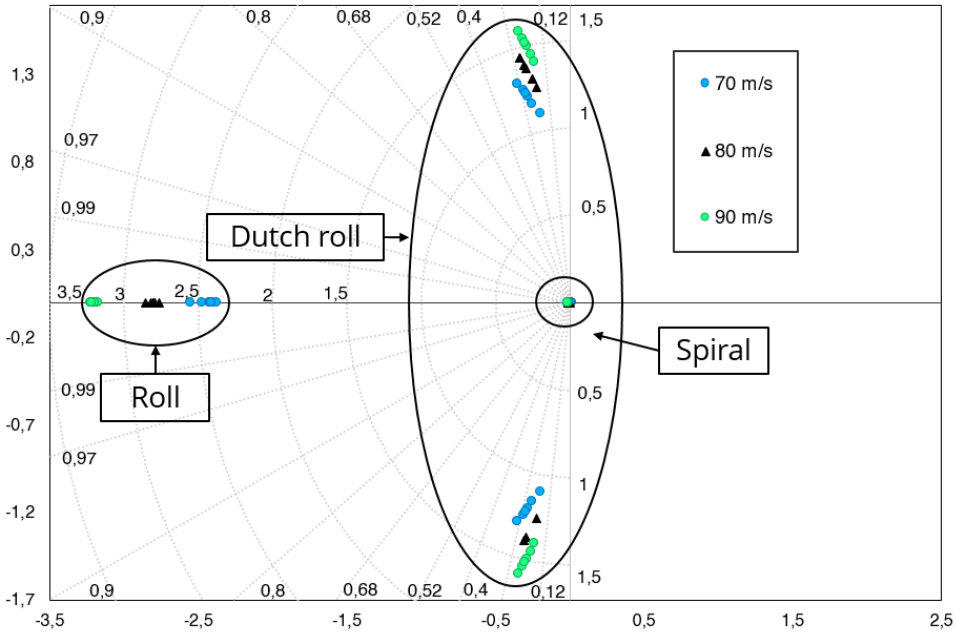

Figure 12 – Lateral modes

An interesting result is given for the SPO when varying the thrust. Variation of this mode is not given for thrust in a conventional aircraft as the derivative of the pitching moment with respect to the angle of attack does not depend on the thrust setting, so the contribution of thrust to the pitching moment is either neglected with the consideration that the thrust passes through the center of gravity, or taken into account into the coefficient C_{m_0}, which is equal to zero after derivation with α. However, when blowing onto the wing in a DEP aircraft, there will be, as it has been shown, a term depending on both the angle of attack and the thrust setting, so therefore $\frac{dC_m}{d\alpha}^{Int} = f(\alpha, \alpha\delta_x)$

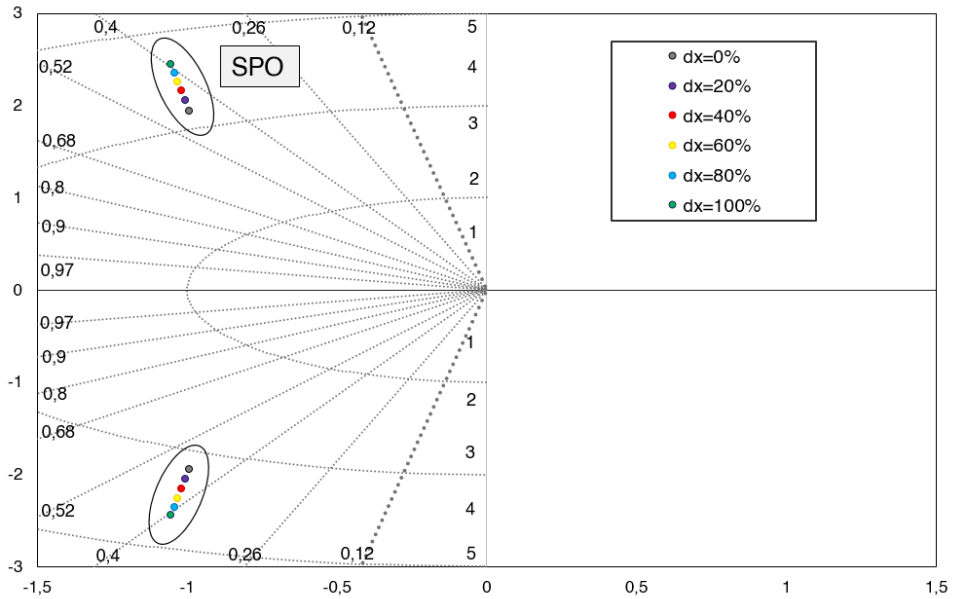

Figure 13 – SPO evolution when varying thrust setting

This term, than in a conventional aircraft is noted as C_{m_α}, has a strong influence on the SPO and therefore there is going to exist an influence of the thrust setting. The root-locus of this mode for the whole range of thrust-setting is shown in figure 13. When increasing thrust, the mode moves away from the real and imaginary lines, becoming slightly faster and less damped.

5. Conclusion

Several aerodynamic models have been integrated and assembled and a tool has been built. Some performance results and HQ have been analyzed through classical methods. Results show the strong effects of DEP on the general aerodynamics of the aircraft, increasing the lift, but also the drag. The interaction has shown the possibility of flying at a lower speed without enforcing the deflection of the flaps. The penalty to be paid is also a strong increase in drag, which makes it necessary to increase the thrust, and also a high pitching moment that obligates to deflect the elevator till its inferior limit. A possible solution for this effect could be to move the wing forward. Overall the interaction allows the aircraft to fly at lower angles of attack for producing the same lift coefficient. Drag could be reduced through vertical size and rudder reduction, by enabling the creation of yaw moment through differential thrust, a possibility that has been already explored in [27]. Whether these advantages alone justify the use of DEP is something that shall be still under discussion.

The validation of the model built is meant through the realization of flight test campaigns with the radio-controlled model DECOL. Several test flights have already been conducted in 2019 and additional flight campaigns are planned. The comparison of results can be used to improve the simulator through correction factors or surrogates models in a loop improving strategy. In addition, the aerodynamic code will be integrated into the software FAST-OAD (Future Aircraft Sizing Tool - Overall Aircraft Design), a package developed jointly by ISAE-SUPAERO and ONERA for the preliminary design, analysis, and optimization of aircraft. The goal is to perform a multidisciplinary optimization under a selection of relevant DEP variables, for instance, the number of engines, their position, the installation angle or the distance to the wingtip, and to propose an optimized strategy for the design and architecture of the control systems, including the allocation of the actuators, and the definition of the control laws. The choices made on the definition of these laws have a direct impact on the dimension of systems and actuators as well as on the performance and HQ, and the objective pursued must be to maximize the possible benefits brought in by DEP. In this final stage, DECOL can be used as an experimental platform to test the performance of the proposed control architectures and laws.

6. Acknowledgments

The author would like to thank ISAE-Supaero, Airbus in the frame of the Chair CEDAR, and the FONISEN Federation for their investment and funding in this project.

7. Contact Author Email Address

david.planas_andres@onera.fr / david.planas-andres@isae-supaero.fr

8. Copyright Statement

References

[1] M. D. Patterson, *Conceptual Design of High-Lift Propeller Systems for Small Electric Aircraft*. PhD thesis, Georgia Institute of Technology, Georgia, USA, aug. 2016.

[2] E. Dillinger, C. Döll, R. Liaboeuf, C. Toussaint, J. Hermetz, C. Verbeke, and M. Ridel, "Handling qualities of ONERA's small business concept plane with Distributed Electric Propulsion," *In 31st ICAS Conference*, Belo Horizonte, Minas Gerais, Brazil, 2018.

[3] P. Schmollgruber, D. Donjat, M. Ridel, I. Cafarelli, O. Atinault, C. François, and B. Paluch, "Multidisciplinary Design and performance of the ONERA Hybrid Electric Distributed Propulsion concept (DRAGON)," *In AIAA SciTech Conference*, Orlando, Florida, USA, 2020.

[4] H. Kim, A. Perry, and P. Ansell, "A Review of Distributed Electric Propulsion Concepts for Air Vehicle Technology," *AIAA/IEEE Electric Aircraft Technologies Symposium*, 2018.

[5] J. Thauvin, *Exploring the design space for a hybrid-electric regional aircraft with multidisciplinary design optimization methods*. PhD thesis, INPT, Toulouse, France, 2018.

[6] P. Schmollgruber, *Enhancement of the conceptual aircraft design process through certification constraints management and full mission simulations*. PhD thesis, ONERA / DTIS, University of Toulouse, Toulouse, France, 2018.

[7] M.-A. G. Tierno, M. P. Cortés, and C. P. Marcos, *Mecánica del vuelo.* Madrid: Garceta, 2nd ed., 2012.

[8] R. S. van Rooyen and M. E. Eshelby, "Assessment of Propeller Influence on Lateral-Directional Stability of Multiengine Aircraft," *Journal of Aircraft*, vol. 18, no. 5, pp. 364–371, 1981.

[9] G. Sachs, "Flight Performance Issues of Electric Aircraft.," *AIAA Atmospheric Flight Mechanics Conference, No. 4727*, 2012.

[10] E. N. Van., *Lateral stability and control of an aircraft equipped with a small vertical tail by differential use of the propulsion systems. Use of co-design methods.* PhD thesis, ISAE-SUPAERO Institut Supérieur de l'Aéronautique et de l'Espace, Toulouse, France, oct. 2020.

[11] S. F. Hoerner, *Fluid dynamic drag.* IOS Press, 1958.

[12] H. S. Ribner, *Propellers in Yaw.* no. NACA report 820, 1945.

[13] *Jane's all the World Aircraft.* Jane's, 2015.

[14] *ATR 72 Airplane flight manual.*

[15] L. Veldhuis., *Propeller Wing Aerodynamic Interference.* PhD thesis, Delft University of Technology, The Netherlands, 2005.

[16] de Vries R., van Arnhem N., S. T., R. Vos, and V. L. L. M., "Aerodynamic Interaction Between Propellers of a Distributed-Propulsion System in Forward Flight.," *Aerospace Science and Technology, Vol. 118*, 2021.

[17] E. Obert, *Aerodynamic design of transport aircraft.* IOS Press, 2009.

[18] A. McDonald and J. R. Gloudemans, "Open Vehicle Sketch Pad: An Open Source Parametric Geometry and Analysis Tool for Conceptual Aircraft Design.," *AIAA 2022-0004. AIAA SCITECH 2022 Forum*, January, 2022.

[19] C. D., N. F., and V. P. D., "A New Approach in Aircraft Vertical Tailplane Design.," *XXII Conference AIDAA*, 2018.

[20] B. McCormick, *Aerodynamics of v/stol flight.* dover publications ed., 1999.

[21] F. Catalano, "On the Effect of an Installed Propeller Slipstream on Wing Aerodynamic Characteristics.," *Acta Polytechnica, no. Vol. 44 No. 3/2004*, 2004.

[22] R. M. H. Stan J Miley and B. J. Holmes, "Wing Laminar Boundary Layer in the Presence of a Propeller Slipstream.," *Journal of Aircraft, vol. 25, no. 7*, 1988.

[23] A. Jameson, *Analysis of Wing Slipstream Flow Interaction.* no. NASA CR-1632, 1970.

[24] E. Obert., "The effect of propeller slipstream on the static longitudinal stability and control of multi-engined propeller aircraft.," *Delf University of Technology*, 1994.

[25] R. Vos and T. Bouquet, "Modeling the Propeller Slipstream Effect on Lift and Pitching Moment," *In 55th AIAA Aerospace Sciences Meeting*, 2017.

[26] C. Roos, G. Hardier, and J.-M. Biannic, "Polynomial and rational approximation with the APRICOT library of the SMAC toolbox," *in Proceedings of the IEEE Multiconference on Systems and Control*, pp. 1473–1478, Antibes, France, October 2014.

[27] E. N. Van, D. Alazard, P. Pastor, and C. Döll, "Towards an Aircraft with Reduced Lateral Static Stability Using Differential Thrust," *In AIAA Aviation Technology, Integration, and Operations Conference*, Atlanta, Georgia, USA, 2018.